Journal Name

Dynamic Article Links ►

Cite this: DOI: 10.1039/c0xx00000x

www.rsc.org/xxxxxx

ARTICLE TYPE

Multianalytical Approach to explain the darkening process of hematite pigment in paintings from ancient Pompeii after accelerated weathering experiments

Maite Maguregui,*[a] Kepa Castro,[b] Héctor Morillas,[b] Josu Trebolazabala,[b] Ulla Knuutinen,[c] Rita Wiesinger,[d] Manfred Schreiner[d] and Juan Manuel Madariaga[b]

Received (in XXX, XXX) Xth XXXXXXXXX 20XX, Accepted Xth XXXXXXXXX 20XX
DOI: 10.1039/b000000x

In this paper, recently excavated *fresco* painting fragments from the House of Marcus Lucretius (Pompeii) and not exposed to the atmosphere since the eruption of the Mount Vesuvius were subjected to a controlled SO_2 atmosphere and high relative humidity. These experiments were conducted in order to simulate under accelerated conditions the possible deterioration of the hematite pigment and plaster. The mineralogical transformation of the polychromy and plaster was monitored using mainly Raman spectroscopy, a non-destructive technique, but also infrared spectroscopy (FT-IR) and scanning electron microscopy energy-dispersive X-ray spectroscopy (SEM-EDS). After different exposure cycles to SO_2, it was confirmed that hematite red pigment (Fe_2O_3) can be reduced into magnetite (Fe_3O_4), which offer the darkened colour to the pigment. While Fe(III) from hematite is reduced into Fe(II) or mixed Fe(III) and Fe(II), the SO_2 can be oxidized (SO_3) and hydrated to suffer a subsequent wet deposition (H_2SO_4 aerosol) causing as well the transformation of calcite into gypsum. Finally, it was assessed that high concentrations of SO_2 can also cause the sulphation of hematite pigment promoting its transformation into paracoquimbite/coquimbite ($Fe_2(SO_4)_3 \cdot 9H_2O$). Moreover, in some areas of the deteriorated painting fragments, non-expected iron (II) sulphate and sulphite species were also identified.

1. Introduction

The mineralogy of the Earth evolves as a consequence of a range of physical, chemical, and biological processes.[1] At large scale, this evolution depends on a sequence of geochemical and petrologic processes, including volcanism and degassing, fractional crystallisation, crystal settling, assimilation reactions, metamorphism, plate tectonics, and associated large-scale fluid-rock interactions. However, at small scale, it is also possible to visualize how minerals and rocks can be transformed due to natural and induced weathering.

More recent is the interest of scientist for the mineralogical alterations produced in artworks and historical buildings. Several studies have been done on this field, for example, the role of oxalates in the transformation of copper minerals in several artworks,[2-4] the chemical transformations of iron oxide phases in CorTen steel sculptures,[5] the mineralogical transformation in historical bricks,[6] the blackening of red lead pigment,[7] the darkening of lead chromate,[8,9] etc.

Special attention has received the mineralogical and colour changes produced in some pigments of the wall paintings from the archaeological site of Pompeii (Italy). Many wall paintings survived the eruption of Mount Vesuvius because the pyroclastic deposits preserved wall paintings and houses until they were excavated. However, since those excavations were made, some pigments have suffered chemical transformation. The most studied chemical transformations of the Pompeian pigments is the blackening or darkening process of red cinnabar (HgS) pigment.[10] Cinnabar pigment can be converted into Hg(0) and S(0) following a photochemical reaction catalysed by chlorine. The metallic mercury particles can be deposited on the original cinnabar surface giving as a result the darkening process of this pigment.[11] In the case of Pompeii, and considering its closeness to the sea, chlorine ions can be deposited on the surface of cinnabar pigment due to the marine aerosol.

Apart from cinnabar, hematite pigment is the most used red pigment in paintings from Pompeian houses. Since ancient times, it has been affirmed that hematite red pigment is a thermically, chemically and mineralogically stable pigment.[12] Hematite

[a]*Department of Analytical Chemistry, Faculty of Pharmacy, University of the Basque Country UPV/EHU, P.O. Box 450, 01006 Vitoria-Gasteiz, Spain. Fax: +34 94 501 30 14; Tel: +34 94 501 30 58; E-mail: maite.maguregui@ehu.es*
[b]*Department of Analytical Chemistry, Faculty of Science and Technology, University of the Basque Country UPV/EHU, P.O. Box 644, 48080 Bilbao,Spain*
[c]*Department of Art and Cultural Studies, University of Jyväskylä, PL 25 FIN-40014, Finland*
[d]*Institute of Science and Technology in Art, Academy of Fine Arts, Schillerplatz 3, A-1010 Vienna, Austria.*

pigment (from the Greek *haimatitis*, which means "blood red") is a variety of red ochre. Like all ochre pigments, it has been used since prehistoric times.[13] In the literature, no references can be found about deterioration processes of red hematite pigment. On the contrary, the thermal transformation of goethite (FeOOH) into hematite (Fe_2O_3) is well referenced. This dehydration process can take place at 250ºC.[14,15] If organic matter is present in the media, maghemite (γ-Fe_2O_3) can be formed, and the transformation product acquire dark red or brown tonality.[16]

Modern polluted atmospheres affect the state of conservation of artworks and historical buildings and can produce also mineralogical changes.[5,6] The beautiful walls and wall paintings from Pompeii have been exposed to the open air since their excavations and subsequently, they have been affected by the high polluted atmosphere of Naples and surroundings. In previous works the blackening process of hematite was identified.[17,18] The presence of blackened hematite red pigment areas were identified in wall paintings from the House of Marcus Lucretius, Pompeii (*insula* IX 3, combination of houses 5 and 24). The in situ screening of those blackened or darkened hematite areas with portable Raman spectroscopy and additional analysis using micro-Raman spectroscopy on cross-sections taken from those areas, revealed the presence of a thin micro-layer of magnetite (Fe_3O_4) together with gypsum and in some cases, the presence of iron (III) sulphate nonahydrate (paracoquimbite and/or coquimbite).[17,18] Additional thermodynamic modelling allowed to establish that the transformation of hematite into magnetite and/or (para)coquimbite is possible after a SO_2 acid gas attack.[18] Similar chemical thermodynamic modelling predictions have been tested with very successful results in other studies.[19,20]

This work presents an accelerated weathering study of recently excavated fragments (around 2x3 cm) painted with hematite and coming from the burial of the House of Marcus Lucretius. The aim was to demonstrate if it is possible to darken the hematite under pollution conditions due to SO_2 gas attack. Painting fragments were subjected to SO_2 impact under high relative humidity conditions in order to simulate the influence of this pollutant in the sulphation process of calcite and hematite [(para)coquimbite formation] and in the transformation of the red hematite into black magnetite. The chemical/mineralogical transformation of hematite pigment and plaster were confirmed using Raman spectroscopy and in some cases Fourier Transform infrared spectroscopy (FT-IR) and scanning electron microscopy energy dispersive X-ray spectroscopy (SEM-EDS).

2. Experimental section

2.1. Instrumentation

A LabRAM ARAMIS Raman confocal microscope by HORIBA Jobin Yvon implementing three excitation lasers (532, 633 and 785 nm) was used to perform the Raman measurements. In this case, and due to the nature of the analysed samples, the 633 and 785 nm laser excitation wavelengths were selected to obtain the best Raman spectral results The treatment of the spectra were carried out using the GRAMS/AI 7.02 (Thermo Fisher Scientific Inc., Waltham, USA) software.

An i-Series FT-IR microscope by Perkin-Elmer (Perkin Elmer, Massachusetts, USA) was used to carry out the IR measurements. Infrared spectra were collected in transmission mode on a compression cell (sampling of crystals from the surface is required for the measurement). Infrared spectra were acquired with a resolution setting of 4 cm^{-1} and 40 scans per acquired spectrum. The spectral range in this case was 4000-600 cm^{-1}. Spectra were acquired with Spectrum™ 5.3.1 software. Data-handling of FT-IR spectra was also carried out using GRAMS/AI 7.02 (Thermo Fisher Scientific Inc., Waltham, USA) software. The interpretation of Raman spectra was done by comparing the sample spectra with the spectra of pure standard compounds contained in the e-VISNICH database of original and decay compounds belonging to the natural, industrial and cultural heritage.[21] Additional databases (RASMIN[22] and RRUFF[23]) were also used in the assignation of Raman spectra. For the infrared spectra interpretation, the obtained spectra were compared with the spectra of pure standard compounds contained in the e-VISART infrared database.[24]

A scanning electron microscope (EVO®40, Carl Zeiss NTS GmbH, Germany) coupled to an energy dispersive X-ray detector (X-Max, Oxford Instruments, Abingdon, Oxfordshire, UK) was used for electron image acquisitions and elemental composition determinations of the samples. As the samples were partially conductive due to their high iron content, they were not coated with carbon or gold in order to avoid interferences in the EDS analyses. The elemental analysis was carried out using an 8.5 mm working distance, a 35° take-off angle and an acceleration voltage of 20 KV. An integration time of 50 s was employed to improve the signal to noise ratio.

2.2. Description of samples

The accelerated weathering experiments were carried out with three selected wall painting fragments (*fresco* painting fragments like the one that showed hematite blackening process) from the house of Marcus Lucretius. The samples were recovered during the excavation works in 2006-2007. Thus, these fragments had not been exposed to the open air since the year 79 AD when Mount Vesuvius erupted. Model samples were not prepared to perform the accelerated weathering experiments, because the authors of this paper believed that real Roman painting fragments extracted from the same Pompeian house could have similar composition (polychromy and mortar including *intonaco* and *arriccio*) and characteristics comparing with the original painting which suffer the hematite blackening process. To perform the accelerated weathering experiments on artificially prepared wall paintings making a copy of Roman *fresco* paintings recipe will be less realistic than doing the experiments on real Roman *fresco* paintings.

In order to confirm that the selected painting fragments are real *fresco* paintings (calcite used as binder of the pigment grains) including only hematite as pigment and calcite as the plaster of the wall painting, several spectroscopic techniques were used (Raman spectroscopy mainly, but also FT-IR microscopy). Once ensured that these fragments only had in their original composition calcite and hematite (possible silicates could be also present coming from the plaster and sometimes coming from possible deposits of the burial), accelerated weathering experiments were performed.

2.3. Accelerated weathering experiments

The accelerated weathering experiments were carried out in the Institute of Science and Technology in Art (Academy of Fine Arts) in Vienna. For that purpose, a weathering cell or hermetic closed glass box (Fig. 1) was used. The moist air stream with the corrosive gas (SO_2) was generated by using a dry synthetic air flow which was provided by a compressor (Jun-Air, Germany, Model OF301-4B 5) in combination with a pure air generator (Sigma-Aldrich, Austria Nitrox Model 140). The quality of the pure air was guaranteed by using high efficiency pre- and post-desiccant filtration. The flow of dry synthetic air was divided into two separate streams. One part of the dry air stream was humidified in a bottle containing distilled and deionised water, and afterwards combined with the untreated airflow to the desired levels of relative humidity (RH). The desired amount of acidifying gases (SO_2 in this case, 98% purity) was batched to this humidified air stream. The humidified air stream and the selected amount of SO_2 passed through a tube to the weathering cell or hermetic closed glass box (see Fig. 1).

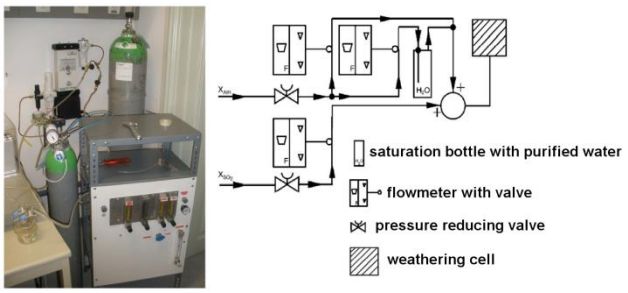

Fig. 1 Assembly of the humidified air stream and SO_2 contribution system and the weathering cell (left) and a scheme of all the system (right).

To design the accelerated weathering experiment, it was taken into account that the wall paintings of the House of Marcus Lucretius with hematite red pigment and calcite have been exposed more or less 166 years to environment of Pompeii since they were discovered. The average concentration of SO_2 in European city atmospheres is more or less 65 μg/m^3 or 25 ppb. The highest amount in Naples during the last 30 years has been 130 μg/m^3 or 50 ppb.[25] Considering that the experimental was conducted in accelerated conditions and taking into account the high amount of SO_2 in the atmosphere near Pompeii, as an initial test 200 ppm (4000 times more than the highest values near Pompeii) of SO_2 were considered to be introduced in the weathering cell.

In the experiments a 90-95% Relative Humidity (RH) was used, in order to achieve the reaction between the water and the SO_2 to generate the sulphuric acid necessary to start the sulphation processes (SO_2 wet deposition).

3. Results and discussion

Different experiments were carried out in order to identify which kind of mineral phases can be formed after an exposure of wall painting fragments to SO_2 and high humidity inside the weathering cell.

In a first experiment, wall painting fragments were introduced in the weathering cell and they were undergone to 200 ppm SO_2 and 90-95 % Relative Humidity (RH) during 24 hours. Afterwards, a non-destructive characterization of the polychromy (hematite) and plaster (calcite) by means of Raman spectroscopy was carried out. Comparing the Raman spectra obtained from the red pigment layer and the plaster before and after the exposure to the SO_2, there were not identify any new mineral phase formed as a consequence of sulphation processes.

Considering this observation, the same exposed wall painting fragments were subjected to an additional weathering cycle of 24 hours, but increasing the amount of SO_2 in the weathering cell up to 400 ppm (8000 times more than the highest value of this acid gas in Naples atmosphere). The Raman analysis performed after this second consecutive experiment, did not revealed the presence of additional mineral phases in the polychromy and plaster.

Taking into account that the formation of sulphates in calcareous materials frequently follows a wet deposition of SO_2 (H_2SO_4 formation in the surface of the wall and subsequent deposition),[26] an extra amount of water inside the weathering cell was included in order to simulate the wet deposition of the SO_2. Therefore, at the bottom of the hermetic closed glass box, a thin layer of Milli-Q water was deposited. Under these conditions, the fragments were exposed 48 hours more to 400 ppm SO_2 and 90-95 % of RH.

After this last chain weathering experiment, the three fragments were analyzed by means of Raman spectroscopy. On the one hand, gypsum ($CaSO_4 \cdot 2H_2O$, showing all their Raman bands, see Fig. 2) was identified in all painting fragments in the *intonaco* (outer part) and also *arriccio* (inner part) layer of the three samples. Gypsum crystals formed in the *arriccio* showed an acicular appearance, while gypsum crystals formed in the *intonaco* showed a rhombohedral appearance (see Fig. 2).

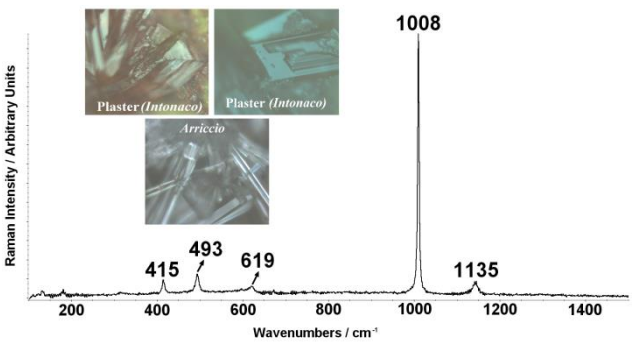

Fig. 2 Rama spectrum and microscopic images (40x objective lens) of gypsum crystals formed in the outer parts of wall painting fragments (*intonaco* layer) and in the inner parts of the wall painting fragments (*arriccio* layer).

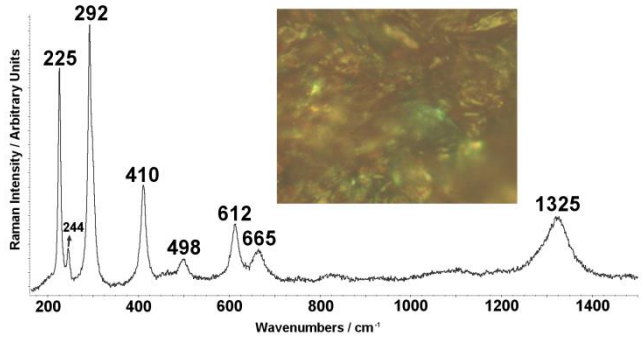

Fig. 3 Raman spectrum of black-greyish crystals on the red polychromy showing Raman bands of hematite (225, 244, 292, 410, 498, 612 and 1325 cm^{-1}) and magnetite (665 cm^{-1}) and a microscopic detail of those crystals (40X objective lens).

Apart from gypsum, additional new mineral phases were identified in the weathered wall painting fragments. In many areas of the red polychromy (hematite), black-greyish areas were identified (see these areas in the microphotography from Fig. 3). Raman measurements performed on those areas showed the presence of an additional Raman band around 660-665 cm^{-1}, apart from Raman bands of hematite (Fe_2O_3) pigment (see Fig. 3). This Raman band can be assigned to magnetite (Fe_3O_4). Magnetite is a mixed oxide of Fe (II) and Fe (III). In many spectra, hematite and magnetite Raman bands appeared together with the main Raman band of gypsum (see Fig. 4).

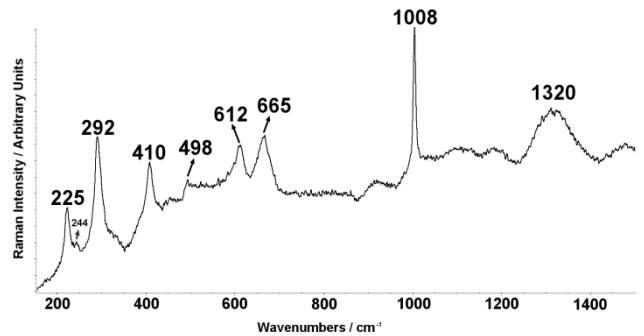

Fig. 4 Raman spectrum of black-greyish crystals on the red polychromy showing hematite (225, 244, 292, 410, 498, 612 and 1320 cm^{-1}), magnetite (665 cm^{-1}) and gypsum (1008 cm^{-1}) Raman bands.

On the surface of the three samples, new white-reddish crystals were also observed. Raman spectra obtained from those crystals showed Raman bands around 220, 280 and 1024 cm^{-1} (see Fig. 5). This Raman feature can be related with an iron (III) sulphate nonahydrate ($Fe_2(SO_4)_3 \cdot 9H_2O$). The spectra acquired in the white-reddish crystals were compared with Raman spectra obtained from a coquimbite mineral which was catalogued and provided by the Natural History Museum of Wien (Naturhistorische Museum). The Raman bands identified in the white-reddish crystals coincide with those obtained from the pure coquimbite mineral (see Fig. 5). Coquimbite mineral Raman spectrum is very similar to that of paracoquimbite. According to literature, paracoquimbite has an additional week band around 501 cm^{-1}.[23, 27] This additional Raman band was not identified in the Raman measurements performed on the weathered surfaces. Apart from the individual presence of coquimbite, this mineral phase was also identified together with the Raman bands of gypsum (see the spectrum at the top of Fig. 6), and also gypsum, hematite and magnetite (see the spectrum at the bottom of Fig. 6 top).

According to these results, the influence of SO_2 in the transformation of hematite pigment into magnetite and coquimbite, together with the sulphation process of the calcite from the *intonaco*, calcite coming from the binder of the fresco painting and calcite from the *arriccio*, was clearly proved. In our previous study,[18] magnetite was pointed as the responsible of the blackening processes of hematite pigment from wall paintings of the House of Marcus Lucretius in Pompeii.

Apart from the Raman evidences, thermodynamic study also predicted that magnetite could be formed as a consequence of SO_2 attack.[18] Moreover, in that work, it was stated that coquimbite and gypsum can be formed as a consequence of SO_2 wet deposition (sulphation of hematite pigment and calcite from the plaster and binder). While SO_2 is oxidized into SO_3 and hydrated/deposited on the surface of the painting as H_2SO_4, hematite red pigment (Fe_2O_3) can be reduced into magnetite (Fe_3O_4). In the same way, hematite can be sulphated and transformed into coquimbite. The presence of hematite, magnetite, gypsum and coquimbite in the same spectrum (see Fig. 6) indicates that in some areas the hematite pigment is not completely transformed into magnetite, but it is partially transformed into magnetite and coquimbite. The present work supports the thermodynamic predictions as well as the Raman evidences about the formation of gypsum, coquimbite and magnetite identified in the wall paintings of the House of Marcus Lucretius.

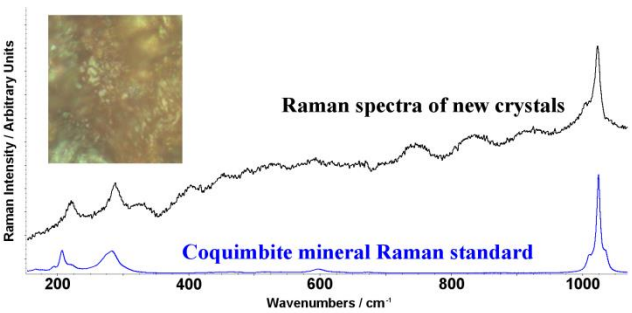

Fig. 5 Raman spectra of the white-reddish crystals and coquimbite mineral and a microscopic detail of the crystals where Raman measurements were performed on painting fragments.

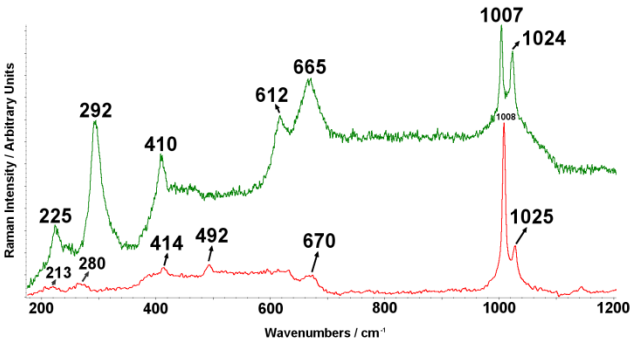

Fig. 6 Raman spectrum of hematite (225, 292, 410 and 612 cm^{-1}), magnetite (665 cm^{-1}), gypsum (1007 cm^{-1}) and coquimbite (1024 cm^{-1}) on the top, and Raman spectrum of gypsum (414, 492, 670 and 1008 cm^{-1}) and coquimbite (213, 280 and 1025 cm^{-1}) on the bottom.

Apart from gypsum, magnetite and coquimbite identification, in some Raman spectra two additional Raman bands at 989 and 962 cm^{-1} (see Fig. 7) respectively were identified. These Raman bands were only identified in two spectra among more than 150 Raman measurements done on each exposed fragment. Therefore, it can be affirm that the presence of the compound/compounds linked to these bands is minority with respect to the rest of the compounds (original and newly formed ones) present. With the Raman spectroscopy it is possible to focus specific and individual crystals and detect their Raman scattering. Considering the punctual or low presence of this/these compound/compounds on the measured surfaces, other analytical techniques (i.e. X-Ray diffraction) that give information about the molecular composition of the sample are not going to be able to detect this/these compound/compounds present in a low percentage with respect to the total composition of the sample.

In the mentioned two spectra, the bands at 989 and 962 cm^{-1} appear together with the main band of gypsum (1008 cm^{-1}). The areas where these two Raman bands were identified were analyzed using an energy dispersive X-ray spectrometer. The elements present in these areas were C, O, Mg, Al, Si, S, K, Ca and Fe (see Fig. 8). Elements such as Al, Si, K and Mg can be present in the sample being part of aluminosilicate aggregates that can be present in the plaster of the exposed *fresco* fragments.

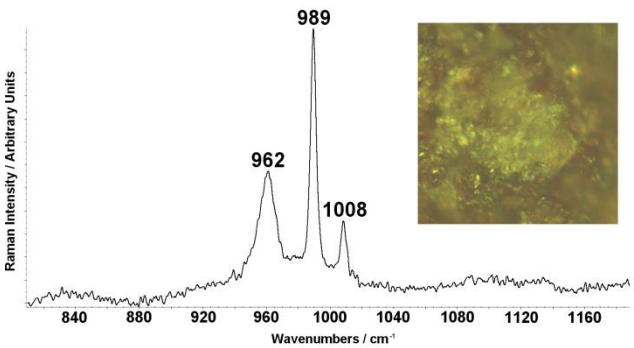

Fig. 7 Raman spectrum of new crystals (see microscopic image detail) showing the main Raman band of gypsum (1008 cm^{-1}) and two Raman bands at 989 and 962 cm^{-1}.

Considering the elemental composition of these crystals and the position of both Raman bands, it can be said that both bands are related to sulphates and/or sulphites.

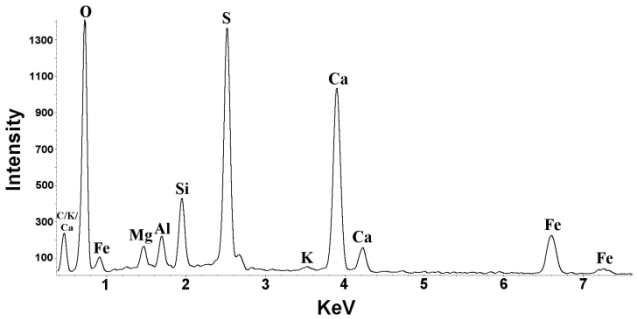

Fig. 8 EDS spectrum of crystal aggregates where 988 and 958 cm-1 Raman bands were identified.

Ettringite $[(CaO)_6(Al_2O_3)(SO_3)_3{\cdot}32H_2O]$ and thaumasite $[Ca_3Si(CO_3)(SO_4)(OH)_6{\cdot}12(H_2O)]$ have their main Raman band around 984 and 989 cm^{-1}.[28] Unfortunately, it is not common or it is not referenced that in an ancient mortar ettringite/thaumasite can be formed as a consequence of an interaction between the mortar and the SO_2.[29] However, it is well-known the formation of ettringite and also thaumasite in concrete and Portland cement.[30] The formation of ettringite happens when gypsum reacts with anhydrous calcium aluminates in a through-solution reaction, but it is difficult to take place in ancient samples. In previous Raman analysis, it was confirmed that the plaster from the weathered wall painting fragments also contain aluminosilicates of calcium and magnesium in its original composition, thus, this aluminosilicates of calcium could react with the sulphates and evolve into ettringite and/or thaumasite.

A recent study[31] also found a Raman band around 980 cm^{-1} together with Raman bands of gypsum and coquimbite in products used in illuminations, lakes and inks. The authors assigned this Raman band to a possible iron sulphate mixture of Fe(II) and Fe(III). Considering this observation, the Raman band at 988 cm^{-1} could belong to an iron sulphate. Rozenite's ($FeSO_4{\cdot}4H_2O$) main band[24] is located at 991 cm^{-1} and szomolnokite's ($FeSO_4{\cdot}H_2O$) main band[24] is located at 989 cm^{-1}. Therefore, in our accelerated weathered samples, the presence of szomolnokite is more probable than that of rozenite.

In the same spectra, together with the band at 989 cm^{-1} and sometimes in presence of the main band of gypsum (see Fig. 7), a band at 962 cm^{-1} can also be observed. This strong band can be assigned to the symmetric stretching vibration of the SO_3^{2-} ion.[32] Some authors related this Raman band with $FeSO_3{\cdot}3H_2O$.[33] The presence of magnetite, indicate that in certain moments of the reaction, iron in two oxidation states (II and III) can be present on the surface of the wall painting fragments. Moreover, the hydrated SO_2 (H_2SO_3) can be partially oxidized into H_2SO_4, but a percentage of H_2SO_3 could remain on the surface of the painting fragments, and therefore, a reaction between H_2SO_3 and reduced hematite (Fe(II)) could take place, giving as a result the formation of iron (II) sulphite with different amount of hydration waters.

To support the Raman analyses, infrared spectra were also collected. Some crystals from the surface of the red hematite paintings were sampled carefully and analyzed by means of FT-IR. All the obtained spectra belonged to gypsum. This is logical,

since the biggest crystals that can be sampled and deposited on the diamond cell are those of gypsum. However, in some white amorphous crystals, in addition to the infrared features of gypsum (infrared band at 3541, 3414, 1683, 1623, 1119, 672 and 601 cm^{-1}) another additional band at 948 cm^{-1} was identified (see Fig. 9). This last IR band can be related with the SO_3^{2-} group vibration.

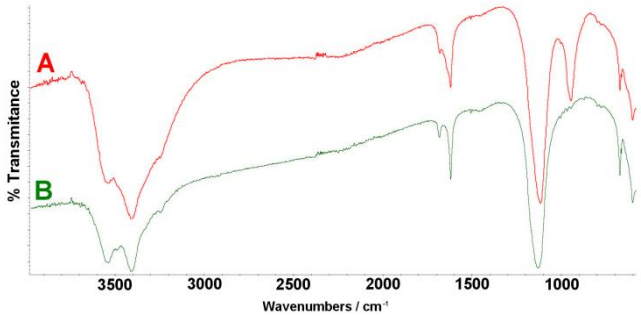

Fig. 9 Infrared spectra of two crystals formed after the accelerated weathering experiments showing the infrared bands of gypsum (B spectrum) and gypsum + strong IR band of sulphite at 948 cm^{-1} (A spectrum).

4. Conclusions

Thanks to the use of accelerated weathering experiments and subsequent non-destructive characterization of samples using spectroscopic techniques such as Raman spectroscopy mainly, but also infrared spectroscopy and energy dispersive X-ray spectroscopy (EDS), it was possible to assess that hematite red pigment (Fe_2O_3) can be reduced into magnetite (Fe_3O_3) in presence of SO_2. This mineralogical transformation is the responsible of the colour change of the pigment from red to darkened red. At the same time, the SO_2 can be oxidized into SO_3 (complementary redox reaction to the hematite reduction) and hydrated on the surface of the painting giving as a result the wet deposition of H_2SO_4. The formed H_2SO_4 can react with the calcite giving as a result the gypsum formation. The sulphuric acid can also react with the hematite giving as a result the sulphation process of iron (III). Under this conditions, the most probable iron (III) sulphate that can be formed is coquimbite ($Fe_2(SO_4)_3{\cdot}9H_2O$). Nevertheless, the possible formation of paracoquimbite, a polymorph of coquimbite, cannot be ruled out.

After conducted all the weathering experiments, it is necessary to highlight the importance of an extra contribution of water in the reaction media to simulate the wet deposition of atmospheric SO_2 pollutant as sulphuric acid, and therefore, to achieve the formation of magnetite, coquimbite and gypsum.

Unexpected results were also obtained, such as the presence of a Raman band at 989 cm^{-1}, which can be related with thaumasite and/or an iron (II) sulphate, probably szomolnokite ($FeSO_4{\cdot}H_2O$). However, the possible formation of other iron (II) sulphates, such as rozenite, etc. should be taken into account. Additionally, the Fe(II) formed in the reduction of the hematite pigment can react on the surface of the painting with the non-oxidized and hydrated H_2SO_3 to form an iron (II) sulphite. The formation of sulphites was also demonstrated with the FT-IR observations, since in some spectra an IR band at 948 cm^{-1} related with SO_3^{2-} group vibration was identified This weathering experiments demonstrate that apart from sulphates, sulphites can be formed after the attack of H_2SO_3 (coming from the hydration of SO_2). In real exposed samples, the common species that are usually detectable after SO_2 impact are sulphates, because with the pass of the time, sulphites can be oxidized into sulphates.

As a final conclusion, it can be said that the proposed accelerated weathering experiments are valid to assess the decaying pathway proposed in a previous study[18] carried out on wall paintings from the House of Marcus Lucretius (Pompeii) to justify the new mineralogical phases formed during the darkening process of the hematite pigment (calcite sulphation from plaster and hematite red pigment transformation into black magnetite and coquimbite) induced by atmospheric pollution.

Acknowledgements

The authors thank the Finnish EPUH project group, especially emeritus Professor Paavo Castren and Docent Antero Tammisto (Helsinki University), for providing the wall painting fragments used for these experiments. The authors also thank to Ira Rabin from the Federal Institute for Materials Research and Testing in Berlin for all the support given, and to the Naturhistorisches Museum (Museum of Natural History) in Vienna for lending the coquimbite mineral. This work was supported by the COST STSM action D-42-6420, the University of the Basque Country UPV/EHU through the UFI Global Change and Heritage (ref UFI11/26) and the Spanish Government (MINECO) through the DEMBUMIES project (ref BIA2011-28418).

References

1 R. M. Hazen, D. Papineau, W. Bleeker, R. T. Downs, J. M. Ferry, T. J. McCoy, D. A. Sverjensky and H. Yang, *Am. Mineral.*, 2008, **93**, 1693-1720.

2 K. Castro, A. Sarmiento, I. Martınez-Arkarazo, J. M. Madariaga and L.A. Fernandez, *Anal. Chem.*, 2008, **80**, 4103-4110.

3 C. Miliani, B. Doherty, A. Daveri, A. Loesch, H. Ulbricht, B. G. Brunetti and A. Sgamellotti, *Spectrochim. Acta A*, 2009, **73**, 587-592.

4 A. Zoppi, C. Lofrumento, N. F. C. Mendes and E. M. Castellucci, *Anal. Bioanal. Chem.*, 2010, **397**, 841-849.

5 J. Aramendia, L. Gomez-Nubla, K. Castro, I. Martinez-Arkarazo, D. Vega, A. Sanz Lopez de Heredia, A. Garcia Ibanez de Opakua, J. M. Madariaga, *J. Raman Spectrosc.*, 2012, **43**, 1111-1117.

6 M. Maguregui, A. Sarmiento, R. Escribano, I. Martinez-Arkarazo, K. Castro and J. M. Madariaga, *Anal. Bioanal. Chem.*, 2009, **395**, 2119-2129.

7 S. Aze, J-M Vallet, M. Pomey, A. Baronnet and O. Grauby, *Eur. J. Mineral.*, 2007, **19**, 883-890

8 L. Monico, G. Van der Snickt, K. Janssens, W. De Nolf, C. Miliani, J. Dik, M. Radepont, E. Hendriks, M. Geldof and M. Cotte, *Anal. Chem.*, 2011, **83**, 1224-1231.

9 L. Monico, G. Van der Snickt, K. Janssens, W. De Nolf, C. Miliani, J. Verbeeck, H. Tian, H. Tan, J. Dik and M. Radepont, *Anal. Chem.*, 2011, **83**, 1213-1223.

10 M. Cotte, J. Susini, N. Metrich, A. Moscato, C. Gratziu, A. Bertagnini and M. Pagano, *Anal. Chem.*, 2006, **78**, 7484–7492.

11 K. Keune and J. J. Boon, *Anal. Chem.*, 2005, **77**, 4742–4750.

12 G.R. Rapp, *Archaeomineralogy*, 2009, Springer-Verlag Berlin Heidelberg, e-ISBN: 978-3-540-78594-1.

13 N. Eastaugh, V. Walsh, T. Chaplin, R. Siddall, *Pigment Compendium, A dictionary of historical pigments*, 2004, Elsevier Buttenworth-Heinemann, Oxford, UK, e-ISBN: 978-1-136-37385-5.
14 M-P. Pomiès, M. Menu, C. Vignaud, *Archaeometry*, 1999, **41**, 275-285.
15 H.D. Ruan, R.L. Frost, J.T. Kloprogge, *Spectrochim. Acta A*, 2001, **57**, 2575-2586.
16 S. Gialanella, R. Belli, G. Dalmeri, I. Lonardelli, M. Mattarelli, M. Montagna, L. Toniutti, *Archaeometry*, 2011, **53**, 950-962.
17 M. Maguregui, U. Knuutinen, K. Castro and J. M. Madariaga, *J. Raman Spectrosc.* 2010, **41**, 1110–1119.
18 M. Maguregui, U. Knuutinen, I. Martínez-Arkarazo, K. Castro and J. M. Madariaga, *Anal. Chem.*, 2011, **83**, 3319–3326.
19 M. Maguregui, A. Sarmiento, I. Martinez-Arkarazo, M. Angulo, K. Castro, G. Arana, N. Etxebarria, J. M. Madariaga, *Anal. Bioanal. Chem.*, 2008, **391**, 1361-1370.
20 M. Pérez-Alonso, K. Castro, M. Alvarez and J. M. Madariaga, *Anal.Chim. Acta*, 2004, **524**, 379-389.
21 M. Maguregui, N. Prieto-Taboada, J. Trebolazabala, N. Goienaga, N. Arrieta, J. Aramendia, L. Gomez-Nubla, A. Sarmiento, M. Olivares, J. A. Carrero, I. Martínez-Arkarazo, K. Castro, G. Arana, M. A. Olazabal, L. A. Fernandez and J. M. Madariaga, *Book of Abstract of the 1st International Congress of Chemistry for Cultural Heritage (ChemCH)*, 2010, p.168
22 http://www.aist.go.jp/index_en.html [last accessed 15 Sept. 2012].
23 http://rruff.info/ [last accessed 26 Sept. 2012].
24 K. Castro, M. Pérez, M. D. Rodríguez and J. M. Madariaga, *Anal. Chem.*, 2003, **75**, 214A-221A.
25 http://www.arpa.veneto.it/home2/htm/home.asp [last accessed on 2010 May 28th [last accessed 19th November 2012].
26 G. Cultrone, A. Arizzi, E. Sebastián and C. Rodriguez-Navarro., *Environ. Geol.*, 2008, **56**, 741-752.
27 Z.C. Ling, A. Wang, *Icarus*, 2010, **209**, 422-433.
28 M. Chollet, M. Horgnies, *Surf. Interface Anal.*, 2011, **43**, 714-725.
29 C. Sabbioni, G. Zappia, J. Aguilera, F. Puertas, K. Van Balen, E.E. Toumbakari, *Atmos. Environ.*, 2001, **35**, 539-548.
30 K.N. Jallad, M. Santhanam, M.D. Cohen, D. Ben-Amotz, *Cement Concr. Res.*, 2001, **31**, 953-958.
31 M. Bicchieri, M. Monti, A. Sodo, G. Piantanida, *1st International Congress ChemCH*, Ravena, Italy, 2010, p.69.
32 V.P. Verma, *Thermochim. Acta*, 1985, **89**, 363.
33 Y-S- Choi, S. Nesic, S. Yound, *Environ. Sci. Technol.*, 2010, **44**, 933-0238.